

# The REM telescope: a robotic facility to monitor the prompt afterglow of gamma ray bursts

L. A. Antonelli<sup>1,\*</sup>, F. M. Zerbi<sup>2</sup>, G. Chincarini<sup>2,3</sup>, G. Ghisellini<sup>2</sup>, M. Rodonò<sup>4</sup>,  
G. Tosti<sup>5</sup>, P. Conconi<sup>2</sup>, S. Covino<sup>2</sup>, G. Cutispoto<sup>4</sup>, E. Molinari<sup>2</sup>, L. Nicastro<sup>6</sup>,  
F. Vitali<sup>1</sup>, and E. Palazzi<sup>7</sup>

<sup>1</sup> INAF, Osservatorio Astronomico di Roma, Monte Porzio Catone, Italy

<sup>2</sup> INAF, Osservatorio Astronomico di Brera, Merate, Italy

<sup>3</sup> Dipartimento di Fisica, Università di Milano Bicocca, Milano, Italy

<sup>4</sup> INAF, Osservatorio Astrofisico di Catania, Catania, Italy

<sup>5</sup> Dipartimento di Fisica, Università di Perugia, Perugia, Italy

<sup>6</sup> CNR, Istituto di Astrofisica Spaziale, Sezione di Palermo, Palermo, Italy

<sup>7</sup> CNR, Istituto di Astrofisica Spaziale, Sezione di Bologna, Bologna, Italy

**Abstract.** Observations of the prompt afterglow of Gamma Ray Burst events are of paramount importance for GRB science and cosmology. In particular early observations at NIR wavelengths are even more promising allowing one to discover and monitor high- $z$  Ly- $\alpha$  absorbed bursts as well as events occurring in dusty star-forming regions. In these pages we present REM (Rapid Eye Mount), a fully robotized fast slewing telescope equipped with a high throughput NIR ( $Z'$ ,  $J$ ,  $H$ ,  $K'$ ) camera (REMIR) and an Optical Slitless Spectrograph (ROSS), dedicated to detect and study prompt IR and optical afterglow. The REM telescope will simultaneously feed REMIR and ROSS via a dichroic. The synergy between the REMIR camera and the ROSS spectrograph makes REM a powerful observing tool for any kind of fast transient phenomena providing an unprecedented simultaneous wavelength coverage on a telescope of this size. Beside its ambitious scientific goals, REM is also technically challenging since it represents the first attempt to locate a NIR camera on such a small telescope.

**Key words.** instrumentation: miscellaneous – telescopes – gamma rays: bursts

## 1. Introduction

REM (Rapid Eye Mount) is a fully robotic fast-slewing telescope primarily designed to follow the early phases of the afterglow of Gamma Ray Bursts (GRB) detected by Space-borne-alert systems such as HETE II, INTEGRAL, AGILE, Swift. REM is

---

*Send offprint requests to:* L. A. Antonelli

\* On behalf of the REM/ROSS team

*Correspondence to:* INAF, Osservatorio Astronomico di Roma, Via Frascati 33, I-00040 Monte Porzio Catone, Italy

currently in its final integration phase and will be installed in the La Silla Observatory (Chile) at the beginning of 2003. REM hosts a NIR (Near Infra-Red) camera covering the 0.95-2.3  $\mu\text{m}$  range with 4 filters ( $Z'$ ,  $J$ ,  $H$ ,  $K'$ ) and ROSS (REM Optical Slitless Spectrograph), a slitless spectrograph covering the range 0.45-0.95  $\mu\text{m}$  with 30 sample points. With these instruments REM will serve as a Rapid-pointing broad band spectro-photometric facility whenever prompt multi-wavelength data are needed.

REM is an ambitious project since it can lead to the discovery and study of the most distant astronomical sources ever observed so far. It is known that roughly a half of the observed GRBs do not show any optical afterglow. At least a part of them can be high- $z$  bursts for which Ly- $\alpha$  absorption dumps all the light at optical wavelengths. Ly- $\alpha$  absorption falls in the REM wavelength range for sources with red-shift between 8 and 15, i.e. any burst in this range can still be detected by REM and its position determined with an accuracy of a few tenth of arcsec. The astrometry will be made available on a time-scale of tenths of second allowing one to observe the transient with larger area telescopes when it is still very bright. A 8-m class telescope equipped with suitable IR spectrographs could collect a high resolution high  $S/N$  spectrum of a source at  $z > 10$ , i.e. the most distance source within or beyond the range of the expected red-shift of reionization ( $8 < z < 20$ ).

The optical slitless spectrograph, ROSS, is as well an outstanding instrument since it will intensively monitor the shape of the optical afterglow continuum and its early temporal behaviour. ROSS will allow to constrain the models for the prompt afterglow emission and will provide, together with REMIR camera, useful information about GRB progenitors and GRB environments.

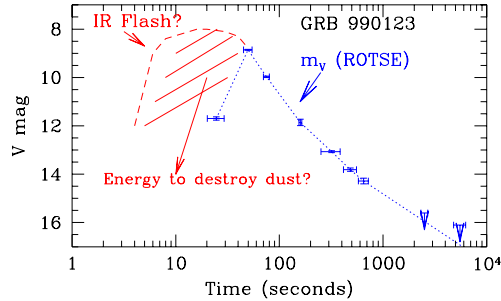


**Fig. 1.** The optical flash of GRB 990123 as seen by ROTSE. Part of the optical UV photons could have been absorbed by dust, in the first part of the emission. After dust has evaporated, the line of sight become extinction free. Since IR photons are much less absorbed by dust, they could pass nearly unabsorbed, resulting in a more prompt emission.

## 2. REM and gamma ray bursts

Gamma Ray Bursts are bright, transient events in the  $\gamma$ -ray sky, unpredictable in time and location, with a typical duration of the order of seconds. The burst event is immediately followed by a fading emission observable at all wavelengths called afterglow. But if 95% of GRBs show a X-ray afterglow almost 50% of them do not show any optical/NIR afterglow at all. In the case in which an optical afterglow has been detected the typically monochromatic flux of its decreases in time as a power law  $F_\nu(t) \sim t^{-\delta}$  with  $\delta$  in the range 0.8-2. Typical magnitudes of optical afterglow detected about one day after the  $\gamma$ -ray event are in the range 19-21. Assuming  $m = 19$  after 24 hours and  $\delta \sim 1.5$ , the expected magnitude after 1 hour is  $\sim 13.8$ . Although we have only two examples of prompt optical/IR emission during the first minutes of the afterglow (GRB 990123 and GRB 020813) they substantially confirmed our estimations of typical early magnitudes of GRBs afterglow. GRB 990123 (Fig. 1) has been detected by the robotic telescope ROTSE about 22 seconds after the  $\gamma$ -ray trigger at  $m \sim 11.7$  and reaching  $m \sim$

8.9 47 seconds after the trigger (Akerlof & McKay 1999). GRB 021004 has been detected by the robotic telescope 48-inch Oschin/NEAT 567 seconds after the  $\gamma$ -ray trigger at  $R = 15.34$  mag (Fox 2002).

REM telescope with its NIR camera is expected to reach magnitude  $H = 15.5$ , 16.04 and 17.11 with exposure times of 5, 30 and 600 seconds respectively ( $S/N = 5$ ). With the ROSS spectrograph a  $V = 14$  point-like source is recorded better than  $10\sigma$  in 1 sec exposures. These numbers suggest that we could detect and study an IR afterglow during the first 2-4 hours even with an exposure time of 5 seconds. This will allow the study of the light curve and eventual flickering in great detail, the detection of possible (even if short) variations from the smooth power-law behavior and the definition of any possible break (Fig. 2). Increasing the exposure time (after the initial phases) to 10 minutes, we can follow typical bursts up to 12 hours, after which larger telescopes can take over. There are many key points we expect that REM can address concerning cosmology and GRBs science.

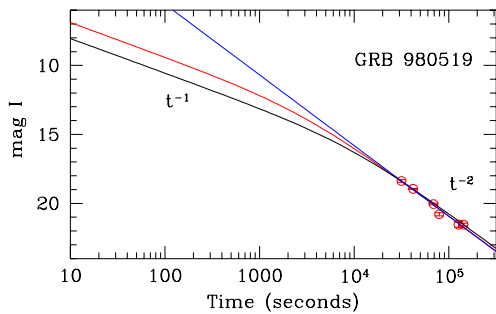


**Fig. 2.** The optical light curve of GRB 980519, with 3 possible extrapolation towards earlier times. Should the early afterglow behave normally (i.e. with a  $t^{-1}$ ) we would have evidence of beaming.

**High- $z$  bursts.** The simultaneous detection in the IR and a non-detection in the optical can directly flag the presence of a high- $z$  object. In fact if a burst is

at high- $z$ , Ly- $\alpha$  absorption dumps all the light at optical wavelengths. Ly- $\alpha$  absorption falls in the REMIR camera wavelength range for sources with redshift between 8 and 15 and through color-color techniques we can select good candidates high- $z$  objects automatically and in real time. Larger telescopes can then point at the target while it is still bright enough for high-dispersion spectroscopic observations in order to study matter distribution and metallicity in the early Universe.

**Reddened bursts.** At low redshifts the lack of optical afterglow can be due to absorption by intervening matter (dust), either in the close vicinity of the burst (if exploded in a dense star forming region whose dust has not been completely destroyed by the burst emission itself), or by dust distributed along the line of sight, even at large distances from the burst site. In this case the infrared light is much less absorbed, and therefore an IR transient can be detected even if the optical is not. From this point of view, the REM telescope, combining the two (IR and optical) datasets, will make possible to estimate the amount of absorption and consequently of the circum-burst medium (e.g. Fig. 3).

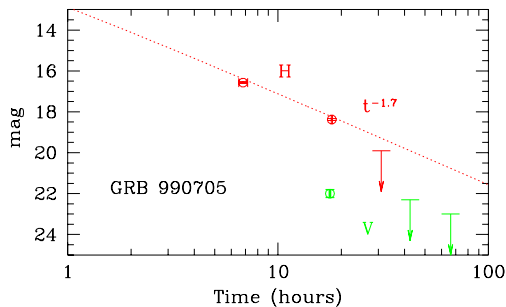


**Fig. 3.** The infrared ( $H$  band) light curve of GRB 990705 (Masetti et al. 2000), with a possible extrapolation towards earlier times and the only detected point in the  $V$  band. The estimated  $V - H$  color is 3.5-4, suggesting either a steep continuum or strong reddening.

**Broad band spectrum.** Even if the theory of afterglow emission (due to synchrotron) is largely accepted, the best constraints we have come from observations performed one or several days after the GRB. It is however possible (if not even likely) that at the beginning of the afterglow the physical conditions (density and temperature) of the shocked material are more extreme and that different emission processes (e.g. Comptonization) are dominant. Increasing the ‘frequency leverage’ is therefore of great importance to better determine the spectrum of the early afterglow in order to better understand the afterglow emission processes.

### 3. REM and ancillary science

As all other robotic facilities dedicated to GRB science, REM reacts to a trigger from a space-borne satellite. This means that for a considerable amount of time REM will be idle in the sense that it will not be pointing any GRB transient. Such a time depends on the number of public triggers eventually provided by missions scheduled to fly during REM operation and it can be estimated around 40% of total REM observing time. During such idle phase REM will serve the community as a fast pointing NIR imager particularly suitable for multi-frequency monitoring of highly variable and transient sources. Some Key-programs of interest for the REM-team have been identified. In particular REM will be used to monitor Flaring Stars, to monitor Blazar and AGN, and, in association with INTEGRAL, to monitor Galactic Black Hole Candidates.

### 4. The hardware

The REM telescope and its instrumentation are currently in the final stage of integration at Brera Observatory (Merate, Italy). The major part of *hardware* has been delivered and is currently be assembled and tested into each subsystem. In this section



**Fig. 4.** The REM telescope.

we give a description of the main characteristics of each subsystem.

#### 4.1. The REM telescope

The REM telescope (Fig. 4) is a Ritchey-Chretien system with a 60 cm  $f/2.2$  primary and a overall  $f/8$  focal ratio mounted in an alt-azimuth mount in order to provide stable Nasmyth focal stations, suitable for fast motions. REM has two Nasmyth focal stations although at first light one will remain idle. At the first focal station a dichroic, working at 45 degrees in the  $f/8$  convergent beam, will split the beam to feed the two first light instruments of the REM telescope: the REMIR camera and the ROSS Spectrograph.

The telescope has been manufactured by Teleskoptechnik Halfmann GmbH in

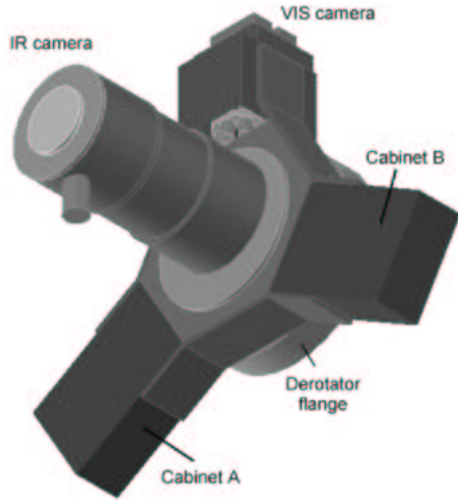


**Fig. 5.** Hexagonal support for instruments.

Augsburg (Germany). Mirrors are made by Carl Zeiss AG (Germany) and they are coated with protected silver to maximize reflection efficiency in such a large (0.45 - 2.3  $\mu\text{m}$ ) wavelength range. The altitude and azimuth motors made by ETEL allows a maximum speed of 12 degree  $\text{sec}^{-1}$  on both axis while the Heidenain encoders (237 steps per arcsec) allows excellent pointing, slewing and tracking precisions.

The mechanical structure has been designed with stiffness in mind, because of the fast motion, but also taking into account the background contamination at NIR wavelength.

The image at the Nasmyth focal station in use is de-rotated and the instrumental flange is designed to receive a load of 250 Kg to be compared to the actual estimated total weight of the instrumentation of about 70 Kg.

The de-rotated Nasmyth focal station will host both the first light instruments REMIR and ROSS. These instrument will be mounted onto an hexagonal instrument flange (Fig. 5), REMIR along the Nasmyth optical axis and ROSS orthogonal to such

axis. The choice of the hexagonal shape allows also to load the control cabinets of the instruments that have to be de-rotated with them. Inside the hexagonal flange the light repartition is done by a dichroic working at  $45^\circ$  in f/8 convergent beam. Since no commercial products of this kind are available the dichroic has been designed at gOlem laboratories of the Brera Observatory (Merate, Italy) and manufactured in collaboration with ZAOT coating laboratories (Milano, Italy). The design phase was aimed to achieve the maximum possible transmission at IR wavelengths (0.95-2.3  $\mu\text{m}$ ) and the maximum possible reflection at Optical wavelength (0.45-0.95  $\mu\text{m}$ ) in the effective working conditions and taking into account of the response of both optical and IR detectors. The adopted solution provides a cut at 0.95  $\mu\text{m}$  and is made of a multi-layer coating of MgF2 and ZnSe on a substrate of IR-SiO<sub>2</sub>. The obtained reflectivity is the average between that at  $42^\circ$  and  $48^\circ$ . The transmission of the device is strictly complementary to the reflectivity since the materials used have negligible absorption. The average reflectivity between 0.45 and 0.90  $\mu\text{m}$  is 0.965 with a minimum of 0.880. The average transmission between 1 and 2.3  $\mu\text{m}$  is 0.972 with a minimum of 0.91.

#### 4.2. The REM IR camera (REMIR)

The REMIR camera (see Vitali et al. 2002 for more details) follows a focal reducer design in order to reform a white pupil in a cold environment for Lyot-stop positioning (see Fig. 6). A filter wheel with 10 positions is located at the reformed pupil allowing one to insert filters and grisms for slit-less spectroscopy or polarimeters in a parallel beam. The camera changes the focal ratio from f/8 to f/5.3 providing a plate-scale of 64.4 arcsec  $\text{mm}^{-1}$  that allows one to position a  $9.9 \times 9.9$  arcmin<sup>2</sup> FOV on a  $512 \times 512$  (18  $\mu\text{m}$  pitch) HgCdTe chip produced by Rockwell.

The REMIR lenses have been designed at gOlem laboratories, (Merate, Italy) and

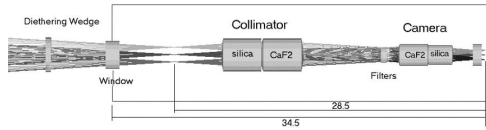


**Fig. 6.** REMIR optical train.

manufactured by Gestione SILO (Florence, Italy). Both collimator and camera (Fig. 6) are made of a Silica-CaF2 doublet (the latter reverse-mounted) with the peculiarity of being more thick than large. Other optical elements are the Cryostat window lens and a field corrector lens near the FPA. The total thickness of the optical design is 345 mm. The image quality is optimal as can be seen in the spot diagrams reported in Fig. 7.

The Filter for the REM-IR camera are standard high performance IR filters. The *J*, *H* and *K*s units have been ordered to Barr Associates Inc. in the framework of the international Consortium lead by University of Hawaii (PI A. Tokunaga). These filters are high performance filters for astronomy manufactured with a special set-up. Beside these standards NIR band we located in REMIR a 1micron filter already used in instruments such as NICS at the Galileo National Telescope, manufactured by Omega Filters. The purpose of this filter is to take profit of the light at wavelength shorter than the *J* band that atmosphere and dichroic let pass and that the HgCdTe chip is still in condition to detect.

The whole camera train is mounted in a dewar, designed and manufactured by IRLabs (Tucson, AZ), and operated in a cool environment. The chip working temperature is 77 K and will be guaranteed at the detector location and at the cold stop position. The optical train is kept at a temperature of about 100-120 K in order to save cooling power. The cryogenics are supported by a Stirling-Cycle cryo-pump made by Leybold AG (Germany) requiring limited maintenance and no need for dewar refilling. A sketch of the mechanical layout of REMIR camera is shown in Fig. 8.

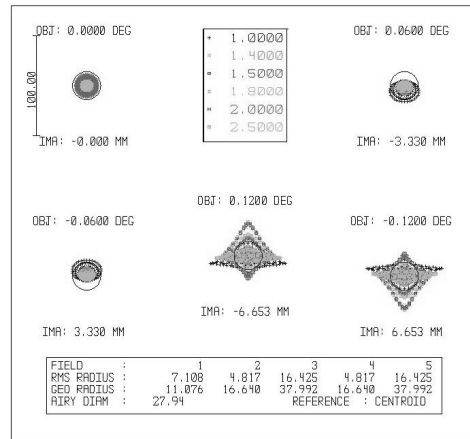


**Fig. 7.** REMIR spot diagrams.

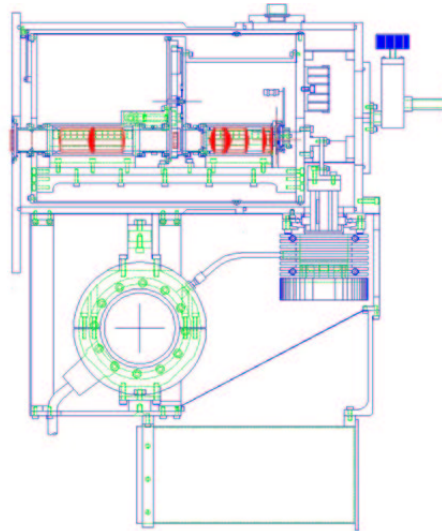


**Fig. 8.** Schematics of the REM-IR cryomechanical system (courtesy of IRLabs).

The chip is a Rockwell HAWAII 1024 × 1024 with 3 out of four quadrant working. Such an unpredictable circumstance (we ordered a chip with a single quadrant working) will allow us to change the working quadrant once the performances degradation of the one in use will no longer be acceptable. The chip is controlled by a Leach Controller and read-out at 1.5 microsecond

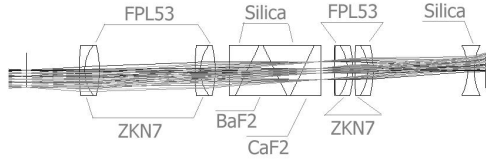


Fig. 9. ROSS optical layout.

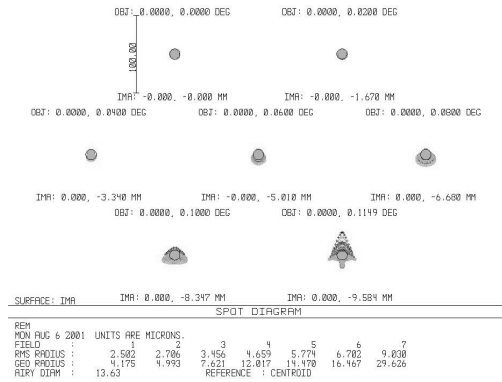


Fig. 10. ROSS spot diagram.

per pixel, this in order to achieve the speed needed for the primary science case.

As a possible upgrade, hence not for first light, we are considering to equip REMIR with a dispersing element to perform slitless spectroscopy also at IR wavelength.

### 4.3. The ROSS spectrograph

With an orthogonal development relative to the REMIR optical axis, REM Nasmyth A will accommodate the slitless spectrograph ROSS. The spectrograph consists of a fore optics which images a pupil at the location of the dispersing element and remaps the focal plane onto the detector unit. The selected detector head is a commercial Apogee AP47 camera hosting a Marconi 47-10 1K×1K 13  $\mu\text{m}$  pitch CCD. The plate scale of the REM telescope (43 arcsec/mm) matches properly with the specifications and allows one to cover a  $9.54 \times 9.54$  arcmin<sup>2</sup> with a scale of 0.56 arcsec pixel<sup>-1</sup>. The fore-optics have been then designed at magnification 1.

The optical layout of the spectrograph is reported in Fig. 9. The collimator is made of a pair of identical ZKN7 - FPL53 separated doublets while the camera is made of two identical FPL53-ZKN7 separated doublets: the pairs differs one from the other. A SILICA window lens with identical curvature on both sides (easier mounting) closes the Apogee detector head. The dispersion is obtained by insertion at the pupil location of an Amici Prism 66 mm long. The prism is made of Silica, BAF2 and CAF2 and it spreads the 0.45-0.95  $\mu\text{m}$  wavelength range on 60 pixels, allowing the recording of 30 2-pixels bins along the range. The optical quality of ROSS is good as can be seen in the spot diagram reported in Fig. 10. The ROSS optics have been designed in house (gOlem laboratories) and manufactured by Gestione SILO (Florence, Italy). At first light the Amici prism will be accompanied by classical *B*, *V*, *R*, *I* imaging filters. As a possible upgrade we are considering a double Wollaston Polarimeter similar to the one presented in Pernechele et al. (2002).

The opto-mechanical layout of ROSS has been kept as simple as possible. The optics are mounted on an optical bench referenced on the telescope side of the instrument hexagon. The compact fore-optics assembly mounts the collimator, the camera and the filter-polarimeter-prism wheel. In front of the detector (shown in figure) a second wheel inserts the plates for differential focus regulation. The ROSS mechanics and optical mountings have been manufactured in house (University of Perugia and INFN laboratories in Perugia).

## 5. Instrument performances

The overall transmission of the REMIR and ROSS optics have been measured during the acceptance tests at gOlem laboratories in Merate. We summarize the expected transmission in Fig. 11; in this figure we show the QE of the ROSS CCD and the REM-IR FPA, the reflection/transmission of the dichroic. The long-dashed line repre-

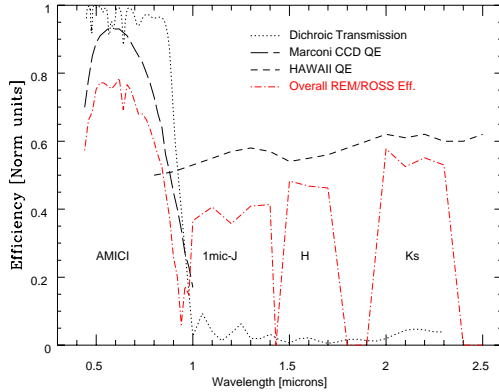


**Fig. 11.** Overall efficiency of the REM assembly. A sign inversion has been operated at the cut-off wavelength of the dichroic.

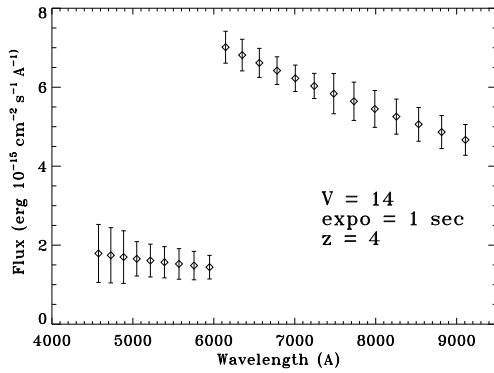


**Fig. 12.** Simulated spectrum of a  $V = 14$  mag GRB optical flash displaying a spectral slope  $F_\lambda \propto \lambda^{-1.25}$  and a Ly- $\alpha$  dropout falling in the optical range due to the source redshift ( $z = 4$ ). The exposure time is 1 second and the  $S/N \sim 4$  below the break and greater than 10 above it.

sents the convolution of all this component with the transmission of the optics and of either the Amici prism, on the optical side, or the ordinary  $J$ ,  $H$ ,  $K_s$  filter transmission. We can see from the figure that even in the most unfortunate circumstance (the  $J$  band) REM transmission always exceeds 30%.

The regime in which REMIR is operated is mainly sky limited and RON and DARK have little effect on the performance. We

computed the limiting magnitudes using the usual formula for  $S/N$  calculations and NTT-SOFI  $J$ ,  $H$  and  $K_s$  filters as a template for REM filters still under procurement. We assume the following average transmissions: 75%, 80% and 85% for  $J$ ,  $H$ ,  $K$  respectively. No predictions have been made for the  $Z$  filter since its transmission will be modulated a posteriori on the cut-on of the HgCdTe chip and the dichroic. The limiting magnitudes computed using these figures are reported in Tab. 1.

In order to evaluate the performance of ROSS, a simulator based on SLIM1 was developed. It is accessible through a (private) Web page with a friendly graphical user interface written in PHP. Results are stored in a browsable SQL database giving access to data, images, spectra, etc. Information about the source in the field are currently taken from the USNO-A2 catalogue. In Fig. 12 is shown the simulation of a GRB event of average magnitude  $R = 14$ , spectral index = 1.25 and  $z = 4$ . Both the break and the high statistical significance are evident.

The REM FOV has been selected to match the typical error-boxes of  $\gamma$ -ray alert systems, e.g. Swift-BAT which has a 4 arcmin  $3\sigma$  errorbox. The need of absolute photometric and astrometric measurements (magnitudes and IR color indices) makes the presence in the FOV of a number of comparison non-variable stars necessary. To check if the FOV is large enough to provide a sufficient number of comparison stars is a task of the REM-Simulator. The REM-Simulator is package, accessible from the REM Web-site, that provides simulated frames of the REM sky at the user defined coordinates and epochs. The principal goal of the REM-simulator is to provide test images to the data reduction software and hence the quality completeness of the simulated image is as high as possible. As regards the number of objects the simulator retrieves the relevant portion of sky from the 2MASS catalogue. Since this catalogue is less deep than the expected REM images the simulator uses the USNO-A1.0 catalogue to complete it.



T (sec)	J		H		K	
	10 $\sigma$	5 $\sigma$	10 $\sigma$	5 $\sigma$	10 $\sigma$	5 $\sigma$
5	15.5	16.3	14.3	15.1	13.1	13.9
30	16.4	17.2	15.2	16.0	14.1	14.8
600	17.3	18.0	16.3	17.1	15.4	16.1

**Table 1.** Limiting magnitudes as a function of the  $S/N$  (10 or 5) and of the pass-band, for the different integration times foreseen in the REM target operation.

### 5.1. REM dome and site

A telescope like REM, specially because of the IR camera, has to be located in a dry and high altitude site with good weather conditions and a high percentage of observing nights. A viable and reliable connection to a large facility accepting Target of Opportunity alerts is in addition an important issue for the success of the project. For this reason we explored possible agreements with existing Observatories with a natural preference for the European Southern Observatory site at la Silla and Cerro Paranal, Chile. An agreement to install REM at la Silla Observatory has been achieved in the framework of the FROST (Fast Robotic Observatory System for Transient), formed by REM and the French Project TAROT-S. REM will be installed at la Silla Observatory at UTM (Zone 19) E 331,235 N 6,762,735, elevation 2,338.80 mt (see the exact location in the map in Fig. 13). The observatory building is already built (Fig. 14) and the telescope first light is expected for Spring 2003.

## 6. REM software and operation

### 6.1. Telescope control software

The robotic character of the REM telescope and the minimization of the need for human intervention is mainly obtained via a robust operation scheme and a highly modular and reliable operation software. The main aim of the project is to deliver a system able to take decisions in a few seconds without any human inter-

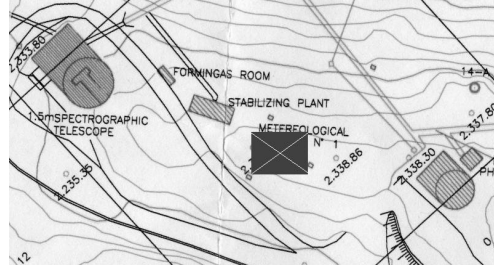


**Fig. 13.** The site where the REM observatory has been built, in between ESO 1.52-m and ESO 1.0-m telescopes at la Silla Observatory, Chile.



**Fig. 14.** The REM dome.

vention. However, an adequate interface to allow a remote human control of operations in case of necessity is developed. In principle, our system can be subdivided from a logical point of view in several subsystems managing various duties of the experiment: the REM Observing Software (REMOS), the REM Telescope Control System (REMTCS), the REM Camera Control Software (REMCCS), the REM Dome Control Software (REMDCS), the REM Environmental Control Software (ECS) and the ROSS control software. All these subsystems can work on different or common CPUs, depending on specific needs. A certain degrees of redundancy is foreseen.

The most general working scenario starts with the reception at the observatory, via an efficient socket connection, of an alert message from the GCN alert system<sup>1</sup>. The message announces the detection of a GRB

<sup>1</sup> <http://gcn.gsfc.nasa.gov/gcn/>

and reports coordinates, error circle radius, time of the event, etc. Then REMOS checks if the possible target satisfies some minimum visibility constraints (hour angle, altitude, sun and moon distance, etc). If these conditions are verified, information from REMECS are retrieved and if observations are possible (humidity, wind, sun altitude, etc., within safety and operational limits) REMOS checks if the system is already observing (another target) or not. If this is the case, and the source is another GRB, a decisional algorithm is applied. Depending on the specific case (Infrared Transient, IT, already discovered, X-ray fluence, favorable sky position, time interval from the GRB, etc. ) eventually a decision is taken. In the positive case (new GRB to be observed) or in case the telescope was observing some lower priority target, REMOS sends a message via socket connection the REMTCS stopping operations and moving the telescope to the new target. As soon as the REMTCS communicates that the telescope is on target the REMOS sends messages to the REMCCS and ROSS to begin observations with some predefined templates. Immediately after the first frames are obtained, they are analyzed by the REM Reduction Software (REMRS) that can, if necessary, send new coordinates to the REMOS, i.e. to better center the target, or modify the observing templates, i.e. in case of peculiarly bright or faint IT.

Of course REMOS also periodically samples the environmental conditions in order to drive the opening or closing of the dome by the REMDCS and stops operation in case some safety alarm is triggered (unexpected intrusion in dome, etc.). Apart from the reaction to a GRB alert, it is possible, by a web based interface, to provide the telescope with coordinate list and observing parameters for any target to be observed for the additional science programs.

### 6.2. AQuA: the REMIR software

The Automatic Quick-Analysis software (AQuA) (see Di Paola et al. 2002 for a de-

tailed description) has been developed and entirely dedicated to the REM data using criteria of high speed, system stability and reliable results in a fully automated way. It runs on a high performance computer with double processor completely dedicated to data handling in order to find transient coordinates and colors. Time sensitive data are quickly distributed via internet to the recipients entitled to receive them (including ToO procedure at larger telescopes) while the bulk of data (2.5 Gbytes of data per night expected) is recorded in a portable storage system. In this scheme the only human intervention needed during normal operation is to change such a removable storage system approximately once every 10 days.

Given the intrinsic rapidity of the phenomena rapid photometry is as essential as the rapid mount drive. Based on a flux model which evolves as a typical GRB we reckon that a measurement of each filter  $Z'$ ,  $J$ ,  $H$  and  $K'$  every 5 seconds in the first observations after targeting is the minimum acceptable frequency. AQuA has been realized in order to satisfy such kind of constraints.

The system is normally working on secondary science activity and waiting for a trigger from the camera acquiring system. When the trigger arrives the system is ready to receive FITS files from the camera directly on a shared disk. It has no command duty with the exception of a line open with the camera control to refine exposure parameters and provide refined coordinates. When the telescope starts to acquire the target the data analysis system will be alerted and it will wait for the first set of images. As the first set of five dithered images will be available on the disk they will be preprocessed in order to obtain one scientific image corrected for bad pixels, flat and sky subtracted. As soon as the final image is ready it will be analyzed by a source detection algorithm and a list of targets will be extracted. Source positions will be compared with catalogues to both perform astrometry and look for pos-

sible candidates. In the following step photometry will be performed on the field and calibrated with 2MASS sources (if present in the field) or using instrumental characteristic (e.g. exposure time vs limiting magnitude). AQuA has been prepared and optimized in order to perform all these operations in few seconds, about the same time needed for the acquiring system to collect another set of images. When a second scientific image becomes available a second source list will be extracted and compared with the previous one looking for variable sources. Furthermore the two images will be subtracted and filtered and the resulting image will be inspected with the detection algorithm and results compared with the previous results. If any source is present in the field the Automatic Quik-Analysis Software will provide the Observation Software with a warning and the camera with a higher exposure time. On the contrary if a transient source will be found the AQuA will provide the OSW with the coordinates. Then coordinates will be delivered in an automatic way via e-mail to existent Alert Networks (e.g. GCN) and/or to a dedicated mailing list (e.g. REM Alert Mail). As soon as positions from the SWIFT optical monitor will be delivered, AQuA will cross check them with REM positions. If an IR transient is found but no optical transient is present in the field, AQuA will activate a ToO to the VLT providing it with transient coordinates. Once the IR source has been found AQuA will command to the camera to use a new filter and then it will perform the analysis on the other images collecting magnitudes in different bands and performing color measures.

Consequently when operated in the Primary science mode, i.e. following GRB triggers, REM will produce 3 classes of output on different time-scales: the coordinate of the IR transient will be available in a few seconds; magnitudes and colors will be available in a few minutes (possibly giving a rough estimate of the distance of the burst via the photometric

red-shift technique); light and color curves will be accurately computed off-line by an extended version of AQuA. Coordinates and colors, especially in the case of a high-redshift burst, are probably the most valuable science output REM can provide.

### 6.3. The ROSS reduction software

Unlike REM, ROSS was not conceived to act as a *real-time* optical detector of the GRB event. The collected ‘dispersed’ images are stored (in FITS format) in a local database (DB) together with all the observation parameters and auxiliary images. Rough spectra are extracted by an automatic process running daytime and saved in a second database as FITS binary tables. A *general log* database is updated and can be used to browse the entire archive. Some column values are identical in the three DBs and are identical to those of the REMIR DB in order to cross identify the observations of the two instruments. Once the data are delivered to Italy, all or selected images can be processed with more care using already available or home made tools. A multi-thread system (under development) manages client connections (through socket) to the DB server and, in addition to data retrieval, allows to perform simple tasks (log output, statistics, graphs, previews, etc.). The DB manager system is based on the open source database system MySQL (TM). The home-written code is mainly in C and PHP.

The ROSS data reduction software can be split into three sections: (a) on-line acquisition and fast-processing, (b) off-line analysis, spectra extraction and archiving, (c) home fine analysis. We already described (c) above. Processes in (a) and (b) are C++ multi-thread pipelines. The on-line processing is activated only for GRB (or other transient) events. As soon as the ROSS control software receives a GRB alert from REMOS, the current observations is stopped and a thread is started in order to create the list of expected objects in the field from a local databases. We plan to use

the not yet released version of the GSC2.3 catalog containing about 1 billion unique GSCII objects. with magnitude limits 18.5 in  $F$  and 19.5 in  $J$ .

When on target, a first image of 1-3 s is accumulated; 1 extra second is required to dump the camera into the computer memory as a FITS image. The image processing thread is started and the accumulation of a second image with the same exposure time of the first is started. The first step of the detection process is the field identification (the pointing in-accuracy is not well defined at the moment but can be significant). Due to the initially unknown position of a reference wavelength in the spectra, we expect a systematic uncertainty of the position of a few arcsec. The real data will help in this respect and the astrometry data will be updated. Then all the objects above a (tunable) threshold are detected and compared with the catalogue list. If no ‘suspect’ is found the image header is updated with the results of the object detection process and a ‘thread’ starts to dump the (raw) image into the DB and to update the observation log. Otherwise any *unidentified* object is investigated in more details; macroscopic properties (intensity, position, shape, etc.) are checked against alert values (mostly seeing and field-crowding dependent). Assuming no simple explanation is found, a variable width PSF fitting is performed and the extracted spectra are fitted with a predefined set of laws. Results are stored in memory and a subprocess performs the dump on file. Also in this case the unknown likely evolving spectral law prevents us from determining the position of the possible transient with an accuracy lower than a few arcsec along the X axis (RA axis - recall the spectra can be considered rectangular in shape, about  $60 \times 3$  pixels and pixel size = 0.6 arcsec).

At this stage a pre-alert is sent to the ROSS control system which in turn alerts REMOS supplying only the relevant info

(position and magnitude) of the transient candidate. Once the second image is available the steps above are repeated. In the case of repeated negative answer the code sends a request to the control system to increase the exposure time. If instead a candidate was found in the first image, a comparison is performed between the two sets of results. Coordinates, fluxes and spectrum properties are compared. Eventually an image subtraction is performed to support the detection. At this time a full alert is sent to REMOS with all the information, including temporal behaviour and spectral properties.

The off-line analysis is performed daytime by an automatic process that analyse images taken during the previous (or earlier) night. This process compares the observation log (which is in a DB) with the spectra DB. Flat-fielding and bias subtraction are performed before to run the object detection and spectra extraction process. As usual, the absolute flux is obtained using standard fields observations. Spectra of the GRB (or other peculiar events) are also copied in a dedicated area for an easier upload to Italy via ftp/http.

*Acknowledgements.* The REM Project has been funded by MURST in the framework of COFIN 2000 and by CNAA in 2000 and 2001. ROSS has been funded by Italian Space Agency in 2000. We gratefully acknowledge the Italian division of AMD who provided us with all computers for the REM observatory.

## References

- Akerlof, C. W., & McKay, T. A. 1999, IAU Circ., 7100, 1
- Di Paola, A., et al. 2002, SPIE, 4847
- Fox, D. W. 2002, GCN Circ., 1564, 1
- Masetti, N., et al. 2000, A&A, 354, 473
- Pernechele, C., et al. 2002, SPIE, 4843
- Vitali, F., et al. 2002, SPIE, 4841
- Zerbi, F. M., et al. 2001, AN, 322, 275